

# Neural Ray-Tracing: Learning Surfaces and Reflectance for Relighting and View Synthesis

Julian Knodt    Joe Bartusek<sup>†</sup>    Seung-Hwan Baek    Felix Heide  
Princeton University

## Abstract

Recent neural rendering methods have demonstrated photo-realistic view interpolation by predicting volumetric density and color with a neural network. Although such volumetric representations can be supervised on static and dynamic scenes, existing methods implicitly bake the scene light transport into a single neural network for a given scene, entangling surface modeling, bidirectional scattering distribution functions, and indirect lighting effects. In contrast to traditional rendering pipelines, this prohibits decomposing scene transport in reflectance and geometry and changing illumination conditions later.

In this work, we explicitly model the light transport between scene surfaces by proposing disentangled neural representations of geometry and reflectance, allowing for efficient inverse rendering. Furthermore, we present a disentangled rendering method inspired by a standard ray-tracing pipeline, inheriting the rendering interpretability for multi-bounce reflection. Combining the neural scene representations and rendering method enables efficient and effective inversion of the rendering equation for inverse rendering. We quantitatively and qualitatively evaluate our method and confirm our approach outperforms existing methods for relighting and view synthesis. Find code under [https://github.com/princeton-computational-imaging/neural\\_raytracing](https://github.com/princeton-computational-imaging/neural_raytracing).

## 1. Introduction

View synthesis and scene reconstruction from a series of images is a fundamental problem in computer vision and graphics. Conventional ray-tracing approaches model physical-light transport, decomposing it into illumination, reflectance, and multi-path scene inter-reflections. These representations are interpretable and offer great editability required for many visual-computing applications such as view synthesis and relighting. However, directly inverting the rendering equation is not trivial in ray-tracing. While remarkable progress has been recently made [14, 14, 30], bypassing the non-differentiable representations and opera-

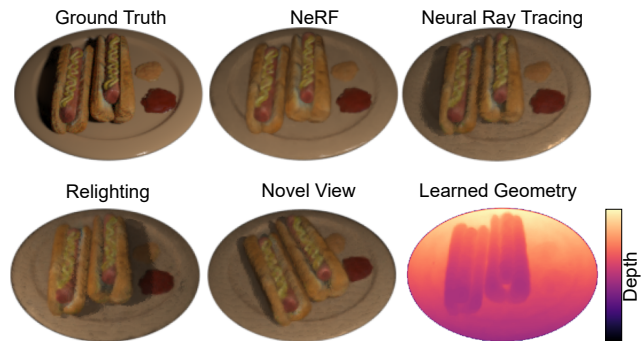


Figure 1. The proposed neural ray-tracing method relies on a novel learned diffuse and non-diffuse BRDF model in conjunction with a SDF-based implicit surface model [28]. This allows us to formulate a path-tracing differentiable rendering pipeline, including ray-casted occlusion. Allowing for decomposable neural ray tracing method is able to recover accurate surface normals as compared to NeRF [13]. In addition, NeRF cannot capture any sort of occlusion, whereas our model is able to accurately predict shadows.

tions in ray tracing is still challenging, limiting its applicability to complex scenes.

Recent advances in neural scene rendering have achieved photo-realistic view synthesis results by encoding the entire scene light transport into a learned volumetric representation [4, 12, 13, 29]. Here, the representations and the rendering procedure are trivially differentiable allowing for modeling complex real-world scenes. However, all light transport components are baked into a higher-dimensional radiance field: because of the implicit radiance representations that these works rely on, light transport, surface representations, and scattering interactions are entangled. This prevents any single component from being recovered or modified without fundamentally altering the others, prohibiting relighting. Recently, attempts to incorporate relighting into existing neural pipelines have been proposed [1, 2, 25]. While these approaches allow for relighting, they rely on dense volumetric sampling for lighting and analysis which limits its variability and rendering efficiency [33].

In this work, we combine the benefits of physically-based ray-tracing and neural scene representations by using neural representations in the middle of a ray-tracing rendering pipeline to disentangle shape, reflectance, and light-

<sup>†</sup>now at Columbia University.

ing. This enables decomposing the baked scene information into each component and hence editing them to accurately relight and simulate a novel view. This provides a bridge between the recent physically-based differentiable rendering [14, 14, 30] and volumetric neural rendering methods [4, 12, 13, 29]

The proposed method exploits neural volumetric geometry model as a signed-distance fields [28] and a novel disentangled reflectance representation for describing a spatially-varying bidirectional scattering distribution function (BSDF). We then present a disentangled rendering method which utilizes the neural representations. Specifically, we partition the optimization space of into the discrete problems of surface estimation, and reflectance estimation by performing physically-based integration and ray-surface intersection during evaluation. This naturally inherits the benefits of physically-based ray-tracing methods for multi-bounce rendering, allowing for efficient simulation of multi-bounce reflection to  $\mathcal{O}(n \log n)$  from  $\mathcal{O}(n^2)$  complexity. We can also interpret our method as incorporating emerging neural scene representations using multi-layer perceptrons (MLP) in a physically-based rendering framework in order to achieve the universality of neural representations [1, 13, 29] and the interpretability of physically-based ray tracing methods. We extensively evaluate the proposed method and demonstrate that we outperform existing methods. In this paper, we make the following contributions:

- We present an end-to-end forward and inverse rendering approach with neural scene reconstructions and ray tracing, allowing for decomposing shape and reflectance in consideration of multi-bounce transport.
- We propose a novel decomposed BSDF model along with efficient path-tracing intersection computation that allows us to recover higher-order bounces quickly.
- The proposed method outperforms existing neural rendering methods qualitatively and quantitatively.

Although the proposed method could be extended to unknown lighting conditions, the scope of this work is known co-located lighting conditions, see also [25], to allow for minimal ambiguity between reflectance and lighting conditions.

## 2. Related Work

### 2.1. Monolithic Scene Representation

With the advent of deep learning and neural networks, a growing body of work has explored methods for scene representations with convolutional neural networks [10, 16, 23] and implicit neural networks [11, 13, 17]. Notably, modeling the scene radiance with a neural implicit function, commonly in the form of a MLP, has proven to be effective, as

demonstrated in NeRF [13]. MLP-based scene modeling integrates light radiance in a volumetric structure and optimizes the volumetric radiance function as a MLP that accurately reproduces a set of reference images, demonstrating learned view-dependent effects. While previous works are effective at novel view synthesis, most of them entangle reflectance, shape, and lighting in a single radiance volume, limiting its usage for physically-accurate scene decomposition [13, 29]. In contrast, we learn physically-based scene representations of shape and reflectance. This enables high-quality, efficient rendering with interpretability, removing black boxes in NeRF.

### 2.2. Geometry-aware Scene Reconstruction

Structure-from-Motion (SfM) has been a golden-standard of reconstructing scene geometry, given a series of images captured at different camera positions [22, 24], however directly using it for synthesizing novel views and relighting is challenging given the sparsity of reconstruction from SfM methods. Recently, implicit differentiable rendering demonstrates effective shape reconstruction based on volumetric signed distance fields [29]. Zhang et al. [32] builds on this geometric representation and employ a spherical Gaussian reflectance model. However, it does not support multi-bounce rendering, which is the core of many physically-based rendering methods. Our work is based on a neural volumetric model, however while previous methods model the entire rendering equation as a black-box neural network, we replace this with explicit integration, inspired by ray tracing to better understand and structure each scene component of geometry, reflectance, and lighting.

### 2.3. Reflectance-aware Scene Representation

With the goal of extending radiance to reflectance, recent works have also explored decomposed modelling of reflectance and volumetric density to enable editable materials and lighting [1, 25]. These works often rely on approximations to volumetric rendering, such as depth-termination prediction. It additionally makes multi-bounce rendering computationally expensive (e.g., 128 TPUs for training [25]). Zhang et al. [33] proposed a neural rendering method to decompose the baked NeRF representation into normals, albedo, and illumination given an unknown illumination condition. All previous work relies on volumetric rendering, demonstrating the lack of representability of discrete structures used in forward rendering pipelines in traditional graphics. Our work attempts to bridge the gap between the successes of neural scene representations for volumetric inverse rendering and physically-based ray-tracing methods for interpretable high-fidelity rendering capability.

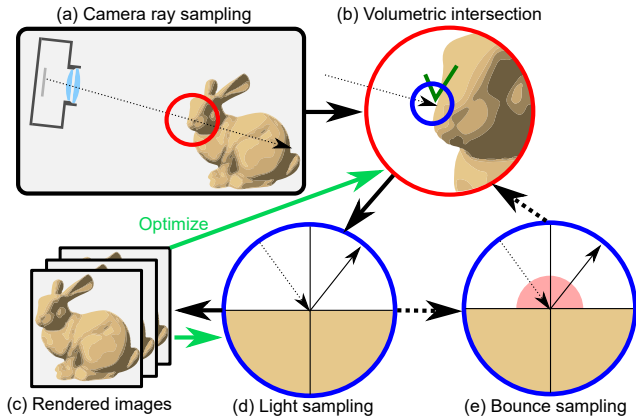


Figure 2. Overview of Neural Ray-Tracing’s pipeline. We ray-march for each pixel in an image, computing the intersection point with the predicted SDF. Then, we sample the direction of the incident light and obtain the reflected energy using its BRDF value. This process is repeated for path tracing, enabling rendering with multiple bounces. Finally, the pixel value is computed using volumetric integration over the RGB at each ray-marched point.

## 2.4. Physically-based Differentiable Ray-Tracing

Ray-tracing has been extensively studied with the goal of generating photorealistic imagery using the rendering equation [18]. Inverting the rendering equation is used to estimate scene compositions and parameters from a given set of input images. Recently, differentiable path-tracing has gained significant interest through frameworks implementing the forward rendering operations in a differentiable manner, so that backpropagation can be applied to optimize over some loss over the rendering pipeline [14, 15, 31]. While these efforts demonstrate promising results, this inversion still faces great challenges. One of the central problems is the conventional representation of shape and reflectance. Shapes are commonly represented as a mesh in existing rendering approaches, imposing non-differentiable geometric discontinuity. While different approaches have been proposed to tackle this problem [6], it is still an open challenge to effectively and efficiently invert transport using the previous scene representations often used for forward rendering. Similarly, analytic reflectance models do not facilitate effective learning via gradient-based optimization, often due to discontinuities over lighting or low-likelihood of sampling specular highlights. In this work, we aim to inherit the benefits of physically-based ray tracing by using its integration and sampling schemes and the differentiable neural scene representations of shape and reflectance.

## 3. Neural Ray-Tracing

The rendering equation proposed by Kajiya [9] has served as the foundation for photo-realistic rendering, mod-

eling both direct and indirect light transport. Specifically, the rendering equation describes the outgoing radiance  $L_o$  coming from a scene point  $\mathbf{x}$  toward a direction  $\omega_o$  as

$$L_o(\mathbf{x}, \omega_o) = L_e(\mathbf{x}, \omega_o) + \int_{\Omega} f(\mathbf{x}, \omega_i, \omega_o) L_i(\mathbf{x}, \omega_i) (\omega_i \cdot \mathbf{n}) d\omega_i, \quad (1)$$

where  $L_e$  and  $L_i$  are the emitted and incident light radiance,  $\omega_i$  is an incident direction,  $f$  is the BRDF, and  $\mathbf{n}$  is the surface normals. All the indirect contribution from other scene points are integrated over the hemisphere  $\Omega$ . Solving this rendering equation is commonly referred as forward rendering and it has been extensively studied in computer graphics. Existing forward rendering methods compute the integral from Eq. (1) by pathtracing using meshes, analytic reflectance and lighting models as scene representation [18]. While being effective for forward rendering, this approach does not lend itself towards solving the inverse problem: estimating scene parameters from observed measurements [15]. Instead, recent neural methods instead take a volumetric rendering approach that bakes all scene light transport into a 5D radiance field [13]. A priori, This prohibits modeling indirect reflection, and complicated interplay between geometry, reflectance, and lighting.

Instead of relying on one of the extremes, we propose neural ray-tracing method which attains the rich light simulation properties of path tracing while resolving the non-differentiable nature of conventional representations by using fully-differentiable neural representations of surfaces and reflectance. Our method defines a differentiable forward rendering function  $\text{Render}()$  which takes the neural representation of shape and reflectance, allowing for iteratively optimizing them with a first-order optimization framework. We start by describing the neural representation of shape and reflectance.

**Disentangled Reflectance** Modeling material reflectance by BSDF,  $f$ , as in Eq. (1) has been extensively studied in computer graphics and vision. Analytical models such as the Phong BSDF [19] and microfacet BSDFs [27] have provided an efficient way of representing real-world reflectance with few parameters. Recently, researchers have proposed neural representations of reflectance that provide differentiability and high representation power with more parameters compared to their analytical counterparts [3, 7]. However, learned models do not provide strong priors on reflectance, therefore directly using it for inverse rendering and accurate recovery is challenging and inefficient. We combine the benefits of both analytical and learned BSDF models by representing reflectance with an analytic Lambertian component and a neural components for the residual learning including specular highlights. This not only maintains the strong representation power of neural representa-

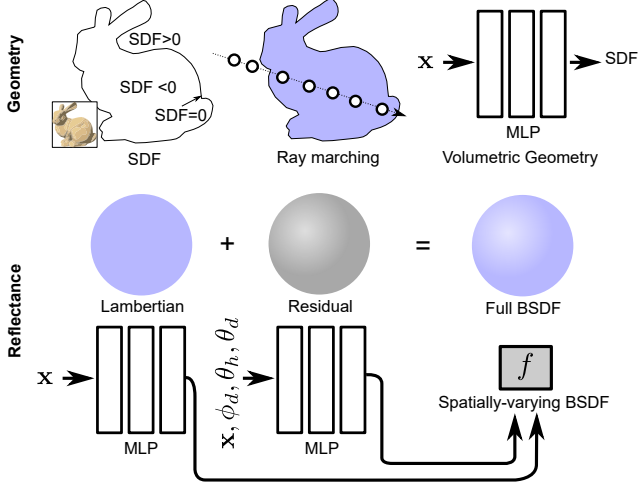


Figure 3. Proposed Neural Scene Representation: Using an SDF modeled as an MLP, we can render high-quality geometry using volumetric integration for primary rays and ray-marching with detached gradients for finding intersections for memory-efficient secondary bounces. For the reflectance, we compose a diffuse Lambertian BxDF with a learned BxDF in order to represent a high-quality spatially-varying BxDF. We combine a learned BxDF with a fully diffuse model in order to enforce correct normals during reconstruction.

tions, but also allows for efficient reconstruction thanks to the parameter efficient Lambertian model. While our model is able to predict albedo in the range  $[-1, 2]$ , a range that includes non-energy preserving values outside of  $[0, 1]$ , it is trained on images in the range  $[0, 1]$ , and the diffuse model provides sufficient initialization to prevent converge to outside that range. In practice, we do not find the energy preservation to affect the reconstruction quality.

Specifically, the Lambertian model component is described as a single diffuse albedo  $k_d(\mathbf{x})$ , modeling foreshortened diffuse reflection  $k_d(\mathbf{x})(\omega_i \cdot \mathbf{n})$ . We note that this model component also indirectly places a *strong prior on the normals*, which is necessary for accurate reconstruction. We model the diffuse color  $k_d(x) \in [0, 1]$  as a Fourier MLP [26] with a sigmoid activation to constrain the value to be positive and energy-preserving. For the learned BxDF component, we introduce an MLP that takes incident and exitant angles with respect to the surface normals and outputs trichromatic reflectance as  $\tanh(\text{MLP}(\mathbf{x}, \phi_d, \cos \theta_h, \cos \theta_d))$ , where  $\phi_d, \theta_h, \theta_d$  are the Rusinkiewicz angles [21]. The Rusinkiewicz angles provide effective angular information and has been proven to be effective in microfacet BxDF models [27]. Note that we use the hyperbolic tangent function for activation to allow for both negative and positive values. This is crucial because residual error of the Lambertian model could be found in any direction. In summary, the proposed reflectance model,

illustrated in Figure 3, is defined as follows

$$f(\mathbf{x}, \omega_o, \omega_i) = f_{\text{Lambert}}(\mathbf{x}) + f_{\text{Learned}}(\mathbf{x}, \phi_d, \theta_h, \theta_d), \quad (2)$$

where  $f_{\text{Lambert}}(\mathbf{x})$  is the Lambertian BxDF defined as  $\sigma(\text{MLP}(\mathbf{x}))$ .  $\sigma$  is the sigmoid function. The function  $f_{\text{Learned}}(\mathbf{x}, \phi_d, \theta_h, \theta_d)$  is the learned residual BxDF defined as  $\tanh(\text{MLP}(\mathbf{x}, \phi_d, \cos \theta_h, \cos \theta_d)) / (\omega_i \cdot \mathbf{n})$ .

### 3.1. Disentangled Neural Rendering

With our neural representations of geometry and reflectance, we now define the forward rendering function  $\text{Render}()$  and describe how to optimize the scene parameters through the rendering function. Ultimately, the goal is to combine pathtracing and neural representations, which imposes a challenge in computational efficiency. Pathtracing requires multiple samples of indirect light path resulting in an exponentially number of MLP evaluations with more bounces. In order to resolve this problem, we use a disentangled alternating rendering approach which allows for effective optimization.

**Direct Reflection and Occlusion Learning** To start the training procedure, we start by focusing on direct reflection and learn the geometric SDF and the Lambertian BxDF:  $\text{SDF}(\mathbf{x}) = \text{MLP}(\mathbf{x})$  and  $f = f_{\text{Lambert}}(\mathbf{x})$ . Specifically, we define the forward rendering function by casting rays toward a camera pixel  $x$  and integrate along the ray using the geometric SDF. For each point  $\mathbf{x}$  along the ray, we sample the direct paths  $\omega'$  to the light sources with known positions. The visibility of the point  $\mathbf{x}$  from the light position is modeled as an MLP with sigmoid activation as  $O(\mathbf{x}, \omega') = \sigma(\text{MLP}(\mathbf{x}, \omega'))$ . We then compute the radiance  $p$  coming from the point  $\mathbf{x}$  toward the pixel  $x$  as

$$p(\mathbf{x}) = \sum_{\mathbf{l} \in L} (\mathbf{n} \cdot \vec{\mathbf{l}}\mathbf{x}) f(\mathbf{x}, \omega_o, \vec{\mathbf{l}}\mathbf{x}) O(\mathbf{x}, \vec{\mathbf{x}}\mathbf{l}) E_{\mathbf{l}}, \quad (3)$$

where  $E_{\mathbf{l}}$  is the radiance for the illumination  $\mathbf{l}$ . Here,  $L$  is the set of light sources, and  $\vec{\mathbf{l}}\mathbf{x}$  is the unit vector from the light source to the point. Given the radiance  $p$ , we can render the pixel value  $I(x)$  using volumetric integration

$$I(x) = \int T(t) \Psi(\text{SDF}(\mathbf{x}(t))) p(\mathbf{x}(t)) dt, \quad (4)$$

where  $\mathbf{x}(t)$  is the sampled point along the emitted ray from the camera pixel  $x$  as  $\mathbf{x}(t) = \mathbf{o} + t\vec{\mathbf{o}}\mathbf{x}$ . The function  $T$  is the transparency function defined as  $T(t) = \exp(-\int_0^t \Psi(\text{SDF}(\mathbf{x}(t))) dt)$ . Here,  $\Psi$  is the volumetric equivalence of an SDF, that is  $\Psi(s) = \frac{1}{2} \exp(\frac{s}{\beta})$  if  $s \leq 0$ , otherwise  $\Psi(s) = 1 - \frac{1}{2} \exp(-\frac{s}{\beta})$ . We assume here that the camera and the illumination are known. The proposed



method relies on this forward rendering function to learn the neural scene representations of the geometric SDF, the Lambertian BSDF, and the occlusion function by solving the following optimization problem

$$\min_{\text{SDF}, f, O} \|I(x; \text{SDF}, f, O) - I_{\text{ref}}(x)\|_2 + R(\text{SDF}),$$

where  $R$  is the eikonal regularization [5] on the surface, that is  $R(\text{SDF}) = \mathbb{E}_{\mathbf{v}_x} [|\|\nabla \text{SDF}(\mathbf{x})\| - 1|^2]$ . Note that the optimization above is performed jointly over all camera views and light sources.

### Residual Reflectance and Geometry-aware Occlusion

In the next optimization step, we increase the model capacity by introducing learned reflectance and geometry-aware occlusion terms. Specifically, we expand the Lambertian-only reflectance term to the full representation in Equation (2) while maintaining the previously-learned Lambertian MLP by only adding the residual MLP with the tangent activation. Next, we increase the capacity of the occlusion model. In the previous stage, our occlusion function  $O$  outputs the value from zero and one with the sigmoid activation, however, there is no guarantee that the learned occlusion  $O$  provides occlusion effect corresponding to the learned geometric SDF. To solve this problem, we first efficiently compute the visibility of the point  $\mathbf{x}$  with respect to the light direction  $\omega'$  by ray casting on the fixed geometry, resulting in a boolean indicator function  $\mathbb{I}_{\text{visible}}(\mathbf{x}, \omega')$ . We then expand the occlusion term as

$$O(\mathbf{x}, \omega') = \sigma(\text{MLP}(\mathbf{x}, \omega'))(\mathbb{I}_v(\mathbf{x}, \omega') + \sigma(k)(1 - \mathbb{I}_v(\mathbf{x}, \omega'))), \quad (5)$$

where  $k$  is a scalar that determines the softness of the ray-cast shadow. The first term  $\sigma(\text{MLP}(\mathbf{x}, \omega'))$  is here the pre-trained model in the first stage. The second term utilizes the visibility function obtained from the fixed geometry and allows for soft shadows. This enables geometric-dependent occlusion modeling. With the updated reflectance and occlusion terms, the inverse procedure then optimizes the learned reflectance and the scalar  $k$  as follows

$$\underset{f, O}{\text{minimize}} \|I(x; \text{SDF}, f, O) - I_{\text{ref}}(x)\|_2. \quad (6)$$

**Multi-bounce Path Tracing** As the next update step, we incorporate multi-bounce reflections via path tracing by exploiting the previously optimized scene representations. Specifically, for every point  $\mathbf{x}$  along the initial ray, we sample directions on the hemisphere. For each sampled direction  $\omega'$ , we find the sign-change region of the optimized SDF which indicates the existence of surface. We then compute the accurate surface intersection  $\mathbf{x}'$  by binary searching the zero set of the SDF within that range. Computational complexity reduces to  $O(N \log N)$  compared to  $O(N^2)$  of NeRV [25]. Furthermore, our approach

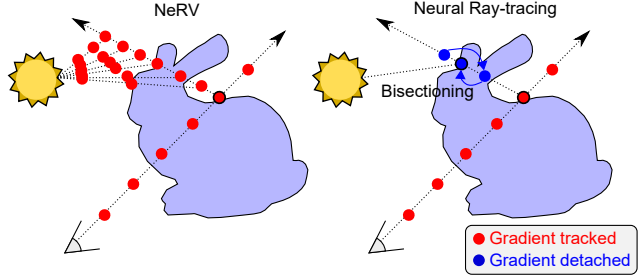


Figure 4. During training, NeRV [25] performs volumetric sampling for both primary and secondary rays to account for multi-bounce reflection. In contrast, our method learns an occlusion MLP at every point given a direction, allowing for efficient training. We fine-tune direct integration with raycasting with detached gradients, and for pathtracing we perform additional bisectioning to find precise intersection points.

is gradient-computation free, resulting in computational efficiency and less memory usage than volumetric integration. See Figure 4. We can then represent the second-bounce contribution to the pixel by accumulating the BSDF evaluations on the original point  $\mathbf{x}$  and the intersection point  $\mathbf{x}'$  as  $f(\mathbf{x}, \vec{\mathbf{x}}\vec{\mathbf{x}}, \vec{\mathbf{x}}'\vec{\mathbf{x}}) \times f(\mathbf{x}', \vec{\mathbf{x}}'\vec{\mathbf{x}}, \vec{\mathbf{l}}\vec{\mathbf{x}}')$ . In this transport estimate, we also include an additional transfer function  $G$  which approximates the joint distribution of the points  $\mathbf{x}$  and  $\mathbf{x}'$  as a MLP with sigmoid activation. That is, the radiance from the point  $\mathbf{x}$  is defined as

$$p(\mathbf{x}) = \sum_{l \in L} \underbrace{\{(\mathbf{n} \cdot \vec{\mathbf{l}}\vec{\mathbf{x}}) f(\mathbf{x}, \omega_o, \vec{\mathbf{l}}\vec{\mathbf{x}}) O(\mathbf{x}, \vec{\mathbf{l}}\vec{\mathbf{x}}) E_l}_{\text{Direct}}} + \underbrace{\sum_{\mathbf{x}'} \{(\mathbf{n} \cdot \vec{\mathbf{x}}'\vec{\mathbf{x}})(\mathbf{n}' \cdot \vec{\mathbf{l}}\vec{\mathbf{x}}') f(\mathbf{x}, \vec{\mathbf{x}}\vec{\mathbf{x}}, \vec{\mathbf{x}}'\vec{\mathbf{x}}) f(\mathbf{x}', \vec{\mathbf{x}}'\vec{\mathbf{x}}, \vec{\mathbf{l}}\vec{\mathbf{x}}') G(\mathbf{x}, \mathbf{x}') E_l\}}_{\text{Indirect}}, \quad (7)$$

where  $\mathbf{n}'$  is the surface normals at the point  $\mathbf{x}'$ . Obtaining the pixel intensity is performed by volumetric integration of Equation (4). We solve the corresponding inverse problem by optimizing the reflectance, occlusion parameters, and the transfer function as

$$\underset{f, O, G}{\text{minimize}} \|I(x; \text{SDF}, f, O) - I_{\text{ref}}(x)\|_2. \quad (8)$$

**Training** We alternately solve the individual inverse problems in Eqs (5,6,8) using the Adam optimizer for all inverse problems. We set the learning rate to  $3 \times 10^{-4}$ , with cosine annealing to a minimum of  $5 \times 10^{-5}$ . All hyper-parameter settings are specified in the Supplemental Document, and a precise specification can be found in the implementation.

We train on the two public datasets from NeRV [25] with single point lights which contain non-collocated point light sources, and also compile our own dataset using a subset



Figure 5. We visualize the decomposition of our model, as compared to the ground truth on two datasets. While the diffuse BSDF is unable to model the underlying BSDF, by combining it with a fully-learned component we are able to learn plausible reconstructions. The albedo is returned prior to any attenuation, and is thus much brighter than the output image.

of the original NeRF scenes, but with collocated point light sources at every view. Collocated point light sources have the benefit that they allow for efficient reconstruction since there are minimal shadows so there is minimal ambiguity between BSDF and lighting conditions. Our method can also reconstruct non-collocated conditions, by introducing shadows using a combination of a learned approximation and raycasting. Our dataset re-renders new configurations of assets used in NeRF [13], consisting of 7 scenes with collocated point lights which will be made available upon acceptance.

#### 4. Assessment

We assess the proposed model by analyzing the light transport decompositions that our approach learns, and how plausible it is for relighting. We train and evaluate on datasets with known illumination, that is the dataset proposed in [25] and a collocated synthetic dataset rendered with collocated illumination on the same synthetic scenes as in [13].

**Relighting and View-Synthesis** With our estimated geometry and reflectance, we are fully equipped to tackle the applications of relighting and view synthesis. We demonstrate relighting under novel conditions in Figure 6. We test our models trained on the collocated light scenes on a test set of unseen 50 novel illumination conditions and 50 novel views, synthesized by orbiting either the point light or the camera around the scene while holding the other in place. Views in these test sets therefore contain shadows, requiring our model to learn a reasonable occlusion model, despite seeing few shadows in the training data. At test time, we compute occlusion using the learned occlusion model and an additional raycasting check, taking advantage

Scene	Hotdog		Lego	
	PSNR <sup>↑</sup>	MS-SSIM <sup>↑</sup>	PSNR <sup>↑</sup>	MS-SSIM <sup>↑</sup>
NeRF	22.75	0.75	18.08	0.66
Ours	25.89	0.87	22.69	0.85
Scene	Materials		Drums	
	PSNR <sup>↑</sup>	MS-SSIM <sup>↑</sup>	PSNR <sup>↑</sup>	MS-SSIM <sup>↑</sup>
NeRF	17.95	0.67	20.73	0.77
Ours	19.14	0.72	22.50	0.83

Table 1. We compare the proposed method against NeRF [13] on our synthesized, relit test scenes, training on collocated point light data. In NeRF, we pass the light vector in addition to the view direction for a fairer comparison. Our method provides better relighting accuracy as compared to NeRF, which cannot explicitly model occlusion.

Scene	Armadillo		Hotdog	
	PSNR <sup>↑</sup>	SSIM <sup>↑</sup>	PSNR <sup>↑</sup>	MS-SSIM <sup>↑</sup>
NeRF+LE	20.35	0.883	19.96	0.868
NeRF+Env	19.60	0.874	19.94	0.863
Bi et al.	22.35	0.894	23.74	0.862
NeRV,NVF	22.14	0.897	23.93	0.863
Ours	25.11	0.883	26.19	0.868

Table 2. We compare results against recent neural rendering methods under known lighting conditions, see text, on the single point-light dataset from [25], with additional results in the Supplemental Document.

of the geometry of our model. Our model is able to accurately recover shadows under a variety of different lighting conditions, as well as free-view movement. Notably, the shadows are consistent across different views, and change in reflectance match the ground truth. In Table 1, we report the quantitative performance of our model compared to NeRF [13], confirming the qualitative trends.

**Comparison to Reflectance-Aware Methods** We compare the proposed method to recent neural reflectance methods including NeRV [25] and Bi et al. [1]. In addition, following [25], we also compare against a NeRF variant (noted as NeRF + LE) which combines the viewing direction with a light-embedding created with PointNet [20], to approximate varying light conditions. Note that we do not compare to NeRFactor since the scopes are different. We assume multiple, known lighting conditions for each view, whereas NeRFactor assumes a single, static, but unknown lighting condition. Figure 7 and Table 2 show that our method outperforms existing methods both quantitatively and qualitatively, facilitated by our explicit surface model and smooth spatially-varying BSDF. Bi et al. [1] does not explicitly learn the true shadow, failing on accurate shadow reproducing. It is also worth noting that our method is mem-



Figure 6. We qualitatively compare our method against NeRF [13] on three synthetic scenes. Note the clean shadows produced by our method, especially in the Lego and Drums scenes, as well as the accurate appearance in the relit and novel view instances, especially in the velvet of the chair.

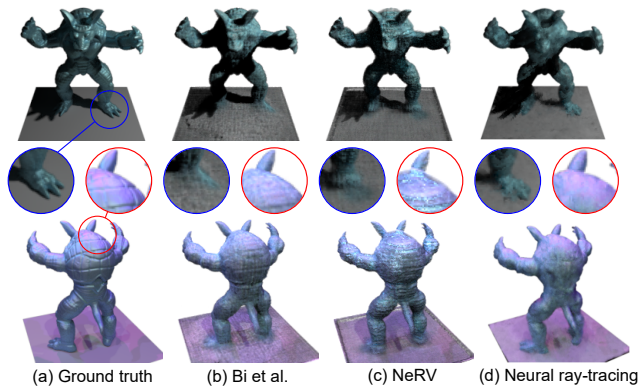


Figure 7. Comparison of our neural ray tracing to Bi et al. [1] and NeRV [25]. We outperform these existing methods by reconstructing accurate details and appearance as shown in the insets. Notably, we more accurately capture the tone of the surface, as highlighted in the insets.

ory efficient training on a single GPU whereas NeRV [25] requires more computing resources, e.g., 128 TPUs in their work. We note that the results of the compared methods are directly copied from the original papers of the authors as

a public implementation was not made available (also confirmed in correspondence with the respective authors).

**Disentangled Reflectance** To validate the effectiveness of the proposed disentangled reflectance model, we evaluate novel view synthesis for models with only diffuse Lambertian and fully-learned residual BSDFs. Specifically, we simply modify Equation (2) to output 1) only the diffuse component, 2) only the learned component, and 3) both components together. Figure 5 and Table 3 show that the full disentangled reflectance model adds a significant increase in PSNR, but alone leads to much lower structural similarity. The results validate that the combination of analytic and learned components offers higher representation power.

### Efficient Multi-Bounce Rendering with Pathtracing

Our method efficiently performs multi-bounce rendering with path tracing. Figure 8 shows the rendered images with direct reflection, second-bounce indirect reflection, and the total rendering which is a sum of the two components. Our multi-bounce path tracing provides indirect illumination in the scene as compared to just the direct illumination. Specifically, for the Lego scene, there is a significant amount of illumination on the roof, because the light is up



Scene	Chair		Hotdog	
	PSNR <sup>†</sup>	MS-SSIM <sup>†</sup>	PSNR <sup>†</sup>	MS-SSIM <sup>†</sup>
Diffuse only	31.27	0.92	26.99	0.86
Learned only	27.74	0.77	25.63	0.81
Both	35.65	0.98	37.70	0.98

Scene	Lego		Drums	
	PSNR <sup>†</sup>	MS-SSIM <sup>†</sup>	PSNR <sup>†</sup>	MS-SSIM <sup>†</sup>
Diffuse only	20.51	0.71	19.60	0.61
Learned only	23.60	0.81	21.57	0.78
Both	29.43	0.95	23.92	0.90

Table 3. Ablation study of our two-component model on multiple synthetic scenes. Rendering by diffuse color alone achieves comparatively high PSNR and MS-SSIM, but the learned-BSDF contribution further improves performance through its ability to model specular reflectance.

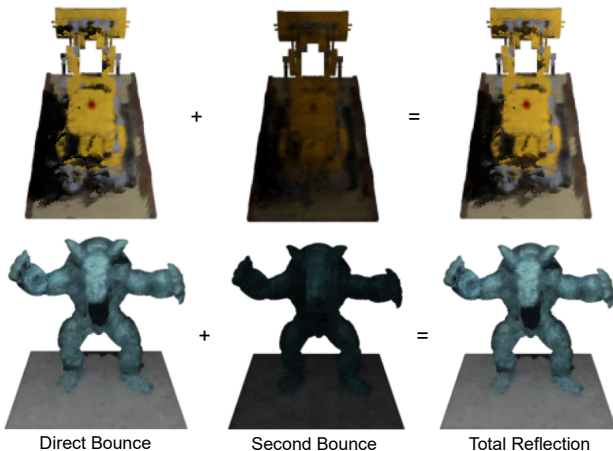


Figure 8. Comparisons of the components of second-order path-tracing. The contribution from second order bounces provides indirect illumination in regions that are not directly visible from the scene illumination sources, see text.

and to the right of the Lego. The light reflects off the tractor claw onto the roof and vice-versa, and thus we see significant illumination. For the Armadillo scene, the light is collocated with the camera, and we see indirect illumination on the face which may be reflection from other components of the face which are strongly illuminated. We achieve this multi-bounce rendering feature in a more efficient manner compared to NeRV [25], see Supplemental Material. Figure 4 describes the difference of our method to NeRV in multi-path rendering. As described previously, we utilize bisectioning and raycasting to facilitate computation- and memory-efficient multi-bounce rendering.

**Experimental Data with Unknown Lighting** To test the applicability of the proposed method on real-world data, where the illumination of the scene is unknown and may vary frame by frame, we recover views from the DTU

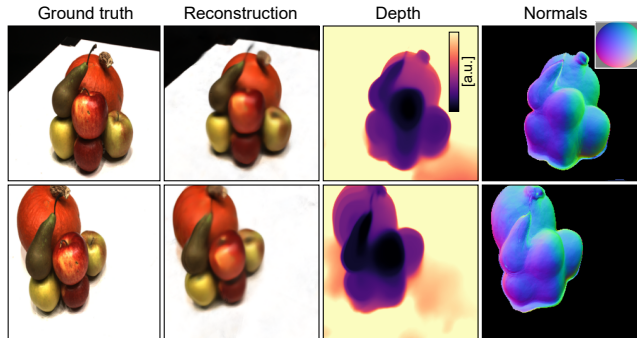


Figure 9. Experimental Reconstruction. When modified to account for unknown lighting, see text, the method is capable of handling experimentally-captured data with unknown lighting, recovering plausible depth and normals, due to the prior over the normals induced by the diffuse BSDF.

dataset. The DTU image data which was captured experimentally in a illuminated environment [8], and we do not use the ground truth illumination measurements. To test whether the proposed method may be extended to unknown illumination scenarios, we modify our method and model spatially-varying lighting as another neural scene representation  $\text{MLP}(\mathbf{x}, \mathbf{z}_i)$  which takes the scene position  $\mathbf{x} \in \mathbb{R}^3$  and the per-image latent vector  $\mathbf{z}_i \in \mathbb{R}^c, c = 64$ , which is optimized during training. The lighting function approximates per-frame scene lighting by returning the intensity and direction of the dominant light for each position. We accurately recover normals and depth as shown in Figure 9. For relighting, see Supplemental Document.

## 5. Conclusion

The proposed explicit modelling of analytic and learned components allows us to directly model light transport, and allows for efficient surface intersections, permitting approximations of soft-shadows, accurate surface reconstruction and fast higher-order light computations. As such, our work bridges the gap between recent MLP-based approaches for neural rendering which rely on a more decomposable pipeline and traditional physically-based rendering approaches. We show that it is possible to combine concepts from conventional, physically-based, inverse-rendering methods with high-fidelity scene representations via neural networks. We hope future neural rendering methods to move towards more explainable learned components, which are currently modelled as block box MLPs in a large body of existing methods in neural rendering, making today’s methods more inefficient, uninterpretable, and challenging to integrate with the rich set of tools and methods developed in traditional rendering approaches – limitations that the proposed method makes steps towards lifting.



## References

- [1] Sai Bi, Zexiang Xu, Pratul Srinivasan, Ben Mildenhall, Kalyan Sunkavalli, Miloš Hašan, Yannick Hold-Geoffroy, David Kriegman, and Ravi Ramamoorthi. Neural reflectance fields for appearance acquisition, 2020. [1](#), [2](#), [6](#), [7](#)
- [2] Sai Bi, Zexiang Xu, Kalyan Sunkavalli, Miloš Hašan, Yannick Hold-Geoffroy, David Kriegman, and Ravi Ramamoorthi. Deep reflectance volumes: Relightable reconstructions from multi-view photometric images, 2020. [1](#)
- [3] Zhe Chen, Shohei Nobuhara, and Ko Nishino. Invertible neural brdf for object inverse rendering. In *Proc. of European Conference on Computer Vision (ECCV)*, Aug 2020. [3](#)
- [4] John Flynn, Michael Broxton, Paul Debevec, Matthew Duvall, Graham Fyffe, Ryan Overbeck, Noah Snavely, and Richard Tucker. Deepview: View synthesis with learned gradient descent, 2019. [1](#), [2](#)
- [5] Amos Gropp, Lior Yariv, Niv Haim, Matan Atzmon, and Yaron Lipman. Implicit geometric regularization for learning shapes, 2020. [5](#)
- [6] Paul Henderson, Vagia Tsiminaki, and Christoph H. Lampert. Leveraging 2d data to learn textured 3d mesh generation, 2020. [3](#)
- [7] Bingyang Hu, Jie Guo, Yanjun Chen, Mengtian Li, and Yanwen Guo. Deepbrdf: A deep representation for manipulating measured brdf. *Computer Graphics Forum*, 39(2):157–166, 2020. [3](#)
- [8] Rasmus Jensen, Anders Dahl, George Vogiatzis, Engil Tola, and Henrik Aanæs. Large scale multi-view stereopsis evaluation. In *2014 IEEE Conference on Computer Vision and Pattern Recognition*, pages 406–413. IEEE, 2014. [8](#)
- [9] James T. Kajiya. The rendering equation. In *Computer Graphics*, pages 143–150, 1986. [3](#)
- [10] Stephen Lombardi, Tomas Simon, Jason Saragih, Gabriel Schwartz, Andreas Lehrmann, and Yaser Sheikh. Neural volumes: Learning dynamic renderable volumes from images. *arXiv preprint arXiv:1906.07751*, 2019. [2](#)
- [11] Lars Mescheder, Michael Oechsle, Michael Niemeyer, Sebastian Nowozin, and Andreas Geiger. Occupancy networks: Learning 3d reconstruction in function space. In *Proceedings of the IEEE/CVF Conference on Computer Vision and Pattern Recognition*, pages 4460–4470, 2019. [2](#)
- [12] Ben Mildenhall, Pratul P. Srinivasan, Rodrigo Ortiz-Cayon, Nima Khademi Kalantari, Ravi Ramamoorthi, Ren Ng, and Abhishek Kar. Local light field fusion: Practical view synthesis with prescriptive sampling guidelines. *ACM Transactions on Graphics (TOG)*, 2019. [1](#), [2](#)
- [13] Ben Mildenhall, Pratul P. Srinivasan, Matthew Tancik, Jonathan T. Barron, Ravi Ramamoorthi, and Ren Ng. Nerf: Representing scenes as neural radiance fields for view synthesis, 2020. [1](#), [2](#), [3](#), [6](#), [7](#)
- [14] Merlin Nimier-David, Sébastien Speierer, Benoît Ruiz, and Wenzel Jakob. Radiative backpropagation: an adjoint method for lightning-fast differentiable rendering. *ACM Transactions on Graphics (TOG)*, 39(4):146–1, 2020. [1](#), [2](#), [3](#)
- [15] Merlin Nimier-David, Delio Vicini, Tizian Zeltner, and Wenzel Jakob. Mitsuba 2: A retargetable forward and inverse renderer. *Transactions on Graphics (Proceedings of SIGGRAPH Asia)*, 38(6), Dec 2019. [3](#)
- [16] Jeong Joon Park, Peter Florence, Julian Straub, Richard Newcombe, and Steven Lovegrove. DeepSDF: Learning continuous signed distance functions for shape representation. In *The IEEE Conference on Computer Vision and Pattern Recognition (CVPR)*, June 2019. [2](#)
- [17] Songyou Peng, Michael Niemeyer, Lars Mescheder, Marc Pollefeys, and Andreas Geiger. Convolutional occupancy networks. *arXiv preprint arXiv:2003.04618*, 2, 2020. [2](#)
- [18] Matt Pharr, Wenzel Jakob, and Greg Humphreys. *Physically Based Rendering: From Theory to Implementation (3rd ed.)*. Morgan Kaufmann Publishers Inc., San Francisco, CA, USA, 3rd edition, Oct 2016. [3](#)
- [19] Bui Tuong Phong. Illumination for computer generated pictures. *Commun. ACM*, 18(6):311–317, Jun 1975. [3](#)
- [20] Charles R. Qi, Hao Su, Kaichun Mo, and Leonidas J. Guibas. Pointnet: Deep learning on point sets for 3d classification and segmentation, 2016. cite arxiv:1612.00593. [6](#)
- [21] Szymon M Rusinkiewicz. A new change of variables for efficient brdf representation. In *Eurographics Workshop on Rendering Techniques*, pages 11–22. Springer, 1998. [4](#)
- [22] Johannes Lutz Schönberger and Jan-Michael Frahm. Structure-from-motion revisited. In *Conference on Computer Vision and Pattern Recognition (CVPR)*, 2016. [2](#)
- [23] Vincent Sitzmann, Justus Thies, Felix Heide, Matthias Nießner, Gordon Wetzstein, and Michael Zollhofer. Deepvoxels: Learning persistent 3d feature embeddings. In *Proceedings of the IEEE/CVF Conference on Computer Vision and Pattern Recognition*, pages 2437–2446, 2019. [2](#)
- [24] Noah Snavely, Steven M Seitz, and Richard Szeliski. Photo tourism: exploring photo collections in 3d. In *ACM Siggraph 2006 papers*, pages 835–846. 2006. [2](#)
- [25] Pratul P Srinivasan, Boyang Deng, Xiuming Zhang, Matthew Tancik, Ben Mildenhall, and Jonathan T Barron. Nerv: Neural reflectance and visibility fields for relighting and view synthesis. *arXiv preprint arXiv:2012.03927*, 2020. [1](#), [2](#), [5](#), [6](#), [7](#), [8](#)
- [26] Matthew Tancik, Pratul P. Srinivasan, Ben Mildenhall, Sara Fridovich-Keil, Nithin Raghavan, Utkarsh Singhal, Ravi Ramamoorthi, Jonathan T. Barron, and Ren Ng. Fourier features let networks learn high frequency functions in low dimensional domains. *NeurIPS*, 2020. [4](#)
- [27] Bruce Walter, Stephen R Marschner, Hongsong Li, and Kenneth E Torrance. Microfacet models for refraction through rough surfaces. *Rendering techniques*, 2007:18th, 2007. [3](#), [4](#)
- [28] Lior Yariv, Jiatao Gu, Yoni Kasten, and Yaron Lipman. Volume rendering of neural implicit surfaces, 2021. [1](#), [2](#)
- [29] Lior Yariv, Yoni Kasten, Dror Moran, Meirav Galun, Matan Atzmon, Ronen Basri, and Yaron Lipman. Multiview neural surface reconstruction by disentangling geometry and appearance, 2020. [1](#), [2](#)
- [30] Cheng Zhang, Bailey Miller, Kai Yan, Ioannis Gkioulekas, and Shuang Zhao. Path-space differentiable rendering. *ACM Trans. Graph.*, 39(4):143:1–143:19, 2020. [1](#), [2](#)
- [31] Cheng Zhang, Bailey Miller, Kai Yan, Ioannis Gkioulekas, and Shuang Zhao. Path-space differentiable rendering. *ACM Trans. Graph.(Proc. SIGGRAPH)*, 39(6):143, 2020. [3](#)

- [32] Kai Zhang, Fujun Luan, Qianqian Wang, Kavita Bala, and Noah Snavely. Physg: Inverse rendering with spherical gaussians for physics-based material editing and relighting, 2021. [2](#)
- [33] Xiuming Zhang, Pratul P Srinivasan, Boyang Deng, Paul Debevec, William T Freeman, and Jonathan T Barron. Nerfactor: Neural factorization of shape and reflectance under an unknown illumination. *arXiv preprint arXiv:2106.01970*, 2021. [1](#), [2](#)